Available online at www.sciencedirect.com
SCIENCE DIRECT®
Journal of Organometallic Chemistry 687 (2003) 451–461
Journal of Organometallic Chemistry
www.elsevier.com/locate/jorganchem

Mechanistic study of palladium catalyzed S–S and Se–Se bonds addition to alkynes

Valentine P. Ananikov [a,*], Michael A. Kabeshov [a,b], Irina P. Beletskaya [b,*], Grigory G. Aleksandrov [c], Igor L. Eremenko [c]

[a] Zelinsky Institute of Organic Chemistry, Russian Academy of Sciences, Leninsky Prospect 47, Moscow 119991, Russia
[b] Chemistry Department, Lomonosov Moscow State University, Vorob'evy gory, Moscow 119899, Russia
[c] Kurnakov Institute of General and Inorganic Chemistry, Leninsky Prospect 31, Moscow 117907, Russia

Received 9 June 2003; received in revised form 31 July 2003; accepted 1 August 2003

Dedicated to Professor J.P. Genet on the occasion of his 60th birthday

Abstract

The mechanistic study of palladium catalyzed S–S and Se–Se bonds addition to alkynes revealed the involvement of dinuclear transition metal complexes in the catalytic cycle. Coordination of alkyne to dinuclear transition metal complex was found to be the rate determining step of the reaction. An unusual phosphine ligand effect increasing the yield of addition reaction was found in the studied system. A new synthetic procedure was developed to perform the catalytic reaction using easily available Pd(II) complex. The scope of the reaction and the reactivity of S–S and Se–Se bonds toward alkynes were investigated. The X-ray structure of the product of S–S bond addition reaction showed favorable geometry for the possible application as a chelate ligand.

Keywords: S–S bond activation; Se–Se bond activation; Addition to alkynes; Palladium complex; Catalytic reaction; ^{77}Se-NMR

1. Introduction

Transition metal catalyzed element–element (E–E) addition to alkynes represents an efficient single step way of the formation of two C_{SP2}–E bonds in a stereoselective manner [1,2]. The process can be performed with 100% atom efficiency, since no waste materials are formed. Several elements have been already investigated (E = B, Si, Sn, Ge, etc.) and it was shown that the catalytic reaction proceeds through the following steps: (1) E–E oxidative addition to the transition metal complex; (2) alkyne coordination to form a π-complex; (3) intramolecular insertion of the coordinated alkyne into the metal–element bond; and (4) reductive elimination resulting in carbon–element (C–E) bond formation and releasing the final product [1,2].

Presently special attention is paid to develop an efficient methodology of S–S and Se–Se bonds addition to alkynes to satisfy increasing demand in modern synthetic organic chemistry [3–6] and material science [7,8]. An excellent work on the subject has been published by Ogawa and coworkers [9]. It was found that $Pd(PPh_3)_4$ catalyzes S–S and Se–Se bonds addition to alkynes with high stereoselectivity [9]. Our recent study has shown that the mechanism of this reaction significantly differs from generally accepted scheme for the other elements [1,2] and involves dinuclear transition metal complexes (Scheme 1) [10]. To the best of our knowledge the study at first pointed out an importance of dinuclear structure of transition metal complex in the catalytic E–E addition reactions. It was also shown that the intermediate dinuclear complexes can be prepared in situ from $Pd(PPh_3)_2Cl_2$ under the action of PhE^- anion, thus replacing traditional $Pd(PPh_3)_4$ catalyst by stable and easily available compound [10]. Without special

* Corresponding authors. Tel.: +7-095-1359094; fax: +7-095-135-5328 (V.P. Ananikov); fax: +7-095-939-3618 (I.P. Beletskaya).
E-mail addresses: val@ioc.ac.ru (V.P. Ananikov), beletska@org.chem.msu.ru (I.P. Beletskaya).

0022-328X/03/$ - see front matter © 2003 Elsevier B.V. All rights reserved.
doi:10.1016/S0022-328X(03)00795-2

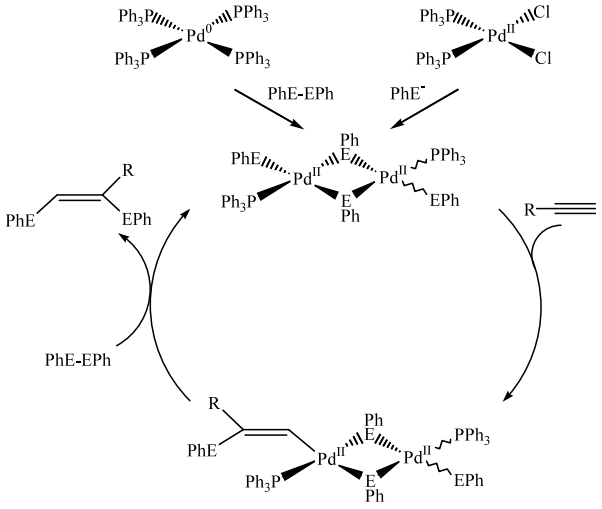

Scheme 1.

treatment $Pd(PPh_3)_2Cl_2$ does not catalyze the reaction [9]. Since only Se–Se bond was considered in our previous study [10] it is of much interest to enlarge the investigation to include more practically important S–S bond addition reaction accompanied with the further development of alternative catalyst design procedure.

In the present article we report additional aspects of the mechanistic study of palladium catalyzed S–S and Se–Se bonds addition to alkynes with the special attention paid to the possible involvement of dinuclear intermediates in the catalytic cycle. A new convenient synthetic procedure was developed to accomplish Ar_2E_2 (E = S, Se) addition to C≡C bond in a simple and efficient way. A comparative study of S–S and Se–Se bonds reactivity toward alkynes was undertaken.

2. Results and discussion

2.1. Dinuclear complexes preparation by oxidative addition and substitution reactions

Oxidative addition of Ph_2E_2 (E = S, Se) to $Pd(PPh_3)_4$ leads to the *trans*- and *cis*-dinuclear derivatives of Pd(II) [11–13]. The complexes can be identified by $^{31}P\{^1H\}$-NMR and their structure was unambiguously established by X-ray analysis [11,13]. The same complexes can by synthesized from $Pd(PPh_3)_2Cl_2$ according to Cl^- substitution reaction by PhE^- (Scheme 2). The PhE^- anion can be generated in situ from Ph_2E_2–$NaBH_4$ (in the presence of MeOH or EtOH) or from PhEH–Et_3N. The measured $^{31}P\{^1H\}$ chemical shifts for the *trans*-/cis-$[Pd_2(EPh)_4(PPh_3)_2]$ were $\delta = 28.1$, 26.6 ppm for **5**, **6** (Fig. 1A) and 30.8, 29.4 ppm for **3**, **4** (Fig. 1B). The same ratio between the low field and high field NMR resonances about 3:1 was measured in both cases (E = S and Se). Most likely, the low field NMR signal corresponds to more stable *trans*-isomer.

For understanding reaction mechanism it is very important to find out how stable the dinuclear palladium complexes are in solution. Merging the toluene solutions of **3**, **4** and **5**, **6** followed by heating at 80 °C for 10 min (Scheme 3) results in intensity decreasing of the ^{31}P-NMR signals corresponding to the parent dinuclear complexes accompanied by appearing of several new resonances in the same spectral region (Fig. 1C).

Splitting ^{31}P-NMR signals with $J(P–P) = 10–15$ Hz (Fig. 1C) clearly indicates lowering the symmetry in the mixed sulfur-/selenium-containing complexes ($m = 1–3$), since at $m = 0$ or $m = 4$ only singlet lines are observed (Fig. 1A and B). As it was confirmed with $^{31}P\{^1H\}$-NMR the same mixed compounds (**8**) are formed upon heating complex **1** (80 °C, 10 min) with the Ph_2S_2–Ph_2Se_2 mixture (Scheme 3).

Therefore, observed SPh–SePh ligands scrambling indicates that dinuclear complexes are labile in solution and could be involved in dissociation and association reactions.

Since dinuclear complexes are important intermediates of the catalytic reaction it is of vital importance to achieve the highest possible yield under the reaction conditions. The quantitative measurements were performed with $^{31}P\{^1H\}$-NMR spectroscopy for both oxidative addition and ligand substitution reactions (Table 1). The NMR study has shown twofold decreasing in intensity of dinuclear complexes signals for the Ph_2S_2–$NaBH_4$ substitution reaction (entry 2, Table 1) compared to oxidative addition (entry 1, Table 1). In the absence of base a very small relative yield of dinuclear complexes was detected using PhSH for chloride ligands substitution (cf. entries 3 and 4, Table 1).

The same yields of complexes **3** and **4** by oxidative addition or PhSH/Et_3N substitution reactions were obtained only after addition of two equivalents of PPh_3 in the latter case (cf. entries 1 and 5, Table 1). It is interesting to note, that further enlarging of the signals intensity was observed with increasing PPh_3 concentration in solution (entries 5–7, Table 1). The same effect has been also observed by adding an excess of PPh_3 to dinuclear complexes obtained by oxidative addition reaction. However, with $NaBH_4$–Ph_2S_2 substitution reaction the intensity of the signals does not accomplish the same level even at large excess of PPh_3.

Therefore, generating PhS^- from the PhSH–Et_3N is more efficient for the substitution reaction than from the $NaBH_4$–Ph_2S_2. For preparing dinuclear complexes the former substitution reaction is as much efficient as the oxidative addition. From the practical point of view using $Pd(PPh_3)_2Cl_2$ as a catalyst precursor possesses several advantages over $Pd(PPh_3)_4$ due to lower cost and higher stability of the Pd(II) complex.

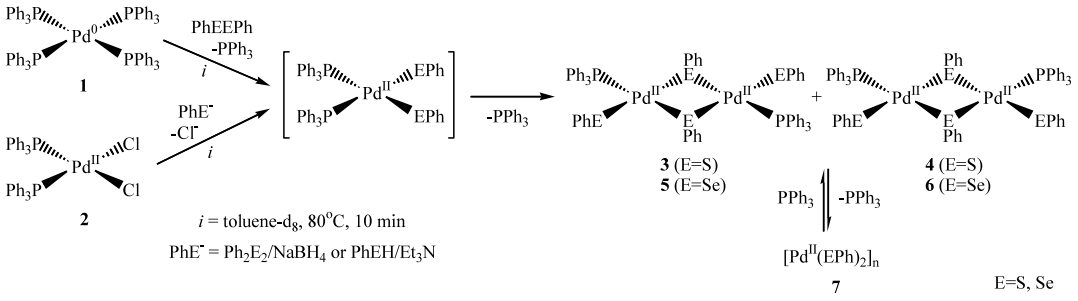

Scheme 2.

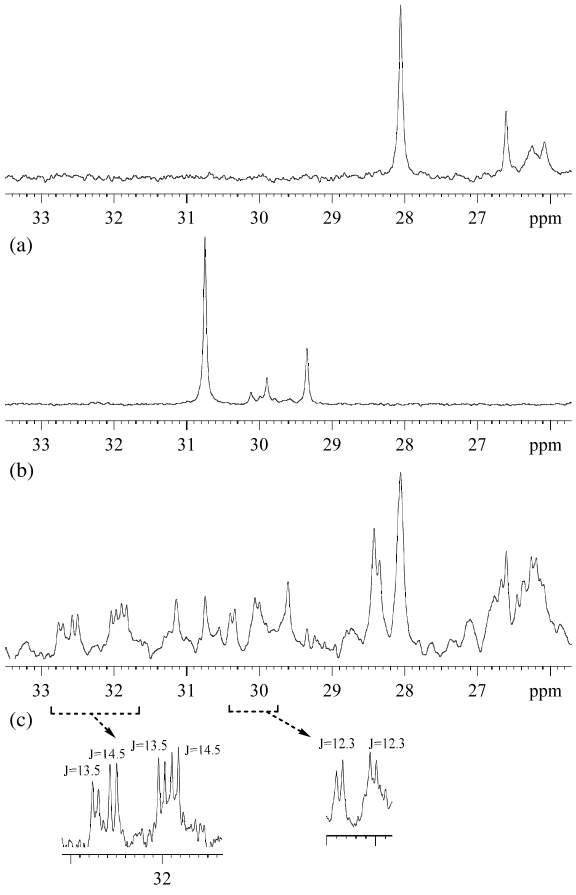

Fig. 1. $^{31}P\{^{1}H\}$-NMR spectra of **5**, **6** (A), **3**, **4** (B) and **8** (C).

2.2. Alkyne insertion into Pd–E bond and C–E reductive elimination (E = S, Se)

Heating the dinuclear complexes **3**, **4** and **5**, **6** in the presence of alkyne (R = CH_2CH_2OH) at 80 °C for 2 h releases the products of Ph_2S_2 and Ph_2Se_2 addition to the triple bond (**9** and **10**, respectively) with the yield about 95% (see caption of Table 2 for structures of **9** and **10**). The products **9** and **10** are formed after alkyne insertion into the Pd–S and Pd–Se bonds followed by C–S and C–Se reductive elimination stages. The reaction of the isolated dinuclear complexes with alkynes gives the same products as the catalytic Ph_2E_2 addition to C≡C bond, thus supporting the proposed reaction mechanism. *Z*-configuration of the products was confirmed with NOESY NMR experiment.

Table 1
The dinuclear complexes formation by oxidative addition and substitution reactions in different conditions [a]

No.	Reaction	Total intensity of **3** and **4** [b]
1	$Pd(PPh_3)_4+Ph_2S_2$	1.0
2	$PdCl_2(PPh_3)_2+NaBH_4+Ph_2S_2$	0.5
3	$PdCl_2(PPh_3)_2+PhSH$	0.2
4	$PdCl_2(PPh_3)_2+PhSH+Et_3N$	0.7
5	$PdCl_2(PPh_3)_2+PhSH+Et_3N+2PPh_3$	1.0
6	$PdCl_2(PPh_3)_2+PhSH+Et_3N+4PPh_3$	1.3
7	$PdCl_2(PPh_3)_2+PhSH+Et_3N+10PPh_3$	1.6

[a] All reactions were performed in toluene solution at 80 °C for 30 min. $PdCl_2(PPh_3)_2$ or $Pd(PPh_3)_4$—8.5×10^{-6} mol, Ph_2S_2—1.7×10^{-5} mol; the ratio $PdCl_2(PPh_3)_2$:PhSH:Et_3N = 1:2:3.
[b] Measured in $^{31}P\{^{1}H\}$ spectra for the signals at δ = 30.8, 29.4 ppm and calculated relative to entry no. 1.

Mixed PhS–PhSe-containing complex **8** also reacts with alkynes (80 °C, 2 h) and besides the above products **9** and **10** gives the compounds **11** and **12** (Table 2). The structure of the products was elucidated with the $^{1}H-^{77}Se$ HMQC NMR method (Fig. 2). The vinyl proton of the compound **10** has two cross-peaks with ^{77}Se signals, a single cross-peak was found for the compounds **11** and **12** and none for the **9**. A known relationship between the spin–spin couplings ^{3}J(Se–

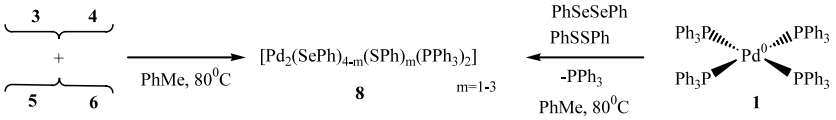

Scheme 3.

Table 2
Alkyne insertion into Pd–E bond of complex **8** and C–E reductive elimination reaction.

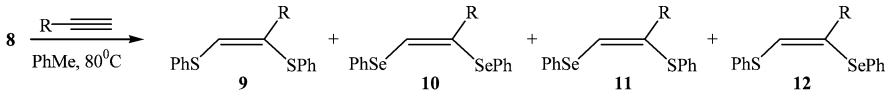

R	Yield, [a] %	9 : 10 : 11 : 12 ratio [b]
-CH_2OH	80	1.1 : 0.8 : 1.0 : 1.0
-CH_2CH_2OH	90	1.2 : 0.9 : 1.0 : 1.0
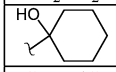	~100	1.2 : 0.8 : 1.0 : 1.0
-$CH_2N(CH_3)_2$	~100	1.3 : 0.9 : 1.0 : 1.0

[a] Determined with NMR spectroscopy. [b] Calculated relative to **11**.

Table 3
Palladium catalyzed Ar_2E_2 addition to alkynes [a]

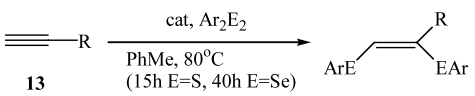

9 ArE=PhS
10 ArE=PhSe
14 ArE=(p-MePh)Se
15 ArE=(p-F Ph)Se

No	Catalyst [b]	Ph_2E_2	Alkyne	Equiv. PPh_3 [c]	Yield, [d] %
1	$Pd(PPh_3)_4$	Ph_2S_2	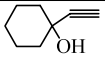 **13-A**	-	70
2	$PdCl_2(PPh_3)_2$/PhSH [1 : 3]	Ph_2S_2	**13-A**	-	0
3	$PdCl_2(PPh_3)_2$/PhSH/Et_3N [1 : 3 : 3]	Ph_2S_2	**13-A**	-	70
4	$PdCl_2(PPh_3)_2$/PhSH/Et_3N [1 : 3 : 3]	Ph_2S_2	**13-A**	2	92
5	$PdCl_2(PPh_3)_2$/PhSH/Et_3N [1 : 3 : 3]	Ph_2S_2	**13-A**	4	98
6	$PdCl_2(PPh_3)_2$/PhSH/Et_3N [1 : 3 : 3]	Ph_2S_2	**13-A**	10	98
7	$PdCl_2(PPh_3)_2$/PhSH/Et_3N [1 : 1.9 : 3]	Ph_2S_2	**13-A**	4	96
8	$PdCl_2(PPh_3)_2$/PhSH/Et_3N [1 : 1.9 : 3]	Ph_2S_2	 **13-B**	-	55
9	$PdCl_2(PPh_3)_2$/PhSH/Et_3N [1 : 1.9 : 3]	Ph_2S_2	**13-B**	4	98
10	$PdCl_2(PPh_3)_2$/PhSH/Et_3N [1 : 1.9 : 3]	Ph_2S_2	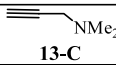 **13-C**	-	83
11	$PdCl_2(PPh_3)_2$/PhSH/Et_3N [1 : 1.9 : 3]	Ph_2S_2	**13-C**	4	96
12	$PdCl_2(PPh_3)_2$/PhSH/Et_3N [1 : 1.9 : 3]	Ph_2S_2	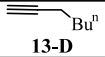 **13-D**	4	98
13	$PdCl_2(PPh_3)_2$/PhSH/Et_3N [1 : 1.9 : 3]	Ph_2S_2	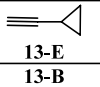 **13-E**	4	96
14	$PdCl_2(PPh_3)_2$/PhSeH/Et_3N [1 : 1.9 : 3]	Ph_2Se_2	**13-B**	6	95
15	$PdCl_2(PPh_3)_2$/PhSeH/Et_3N [1 : 1.9 : 3]	Ph_2Se_2	**13-C**	6	92
16	$PdCl_2(PPh_3)_2$/PhSeH/Et_3N [1 : 1.9 : 3]	Ph_2Se_2	**13-E**	6	94
17	$PdCl_2(PPh_3)_2$/PhSeH/Et_3N [1 : 1.9 : 3]	$(p\text{-MePh})_2Se_2$	**13-B**	6	85
18	$PdCl_2(PPh_3)_2$/PhSeH/Et_3N [1 : 1.9 : 3]	$(p\text{-F Ph})_2Se_2$	**13-B**	6	83

[a] See experimental procedure for details. [b] Molar ratio is given is square brackets. [c] Molar equivalents of PPh_3 relative to palladium catalyst. [d] Determined with NMR spectroscopy, isolated yields for the addition reactions in the presence of PPh_3 were 80-90%.

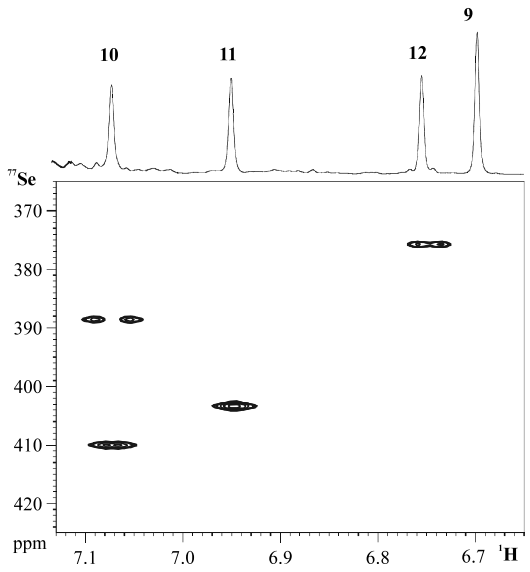

Fig. 2. The ^{1}H–^{77}Se HMQC spectrum of the mixture of **9**–**12** (R = CH_2CH_2OH, $CDCl_3$, 25 °C, 500 MHz ^{1}H).

$H)_{trans} > {}^{2}J(Se–H)_{gem}$ provides an easy route to assign compounds **11** and **12**, since in the former case a larger distance between cross–peak components should be observed (Fig. 2). *Z*-configuration of all the products was confirmed with a 2D NOESY experiment.

Surprisingly, the same **11**:**12** = 1:1 ratio was found for all studied alkynes (Table 2). This might suggest that alkyne insertion and reductive elimination are not the rate-determining stages, otherwise more sensitivity to the substitution effect should be expected. The results are in agreement with the theoretical study of transition metal catalyzed B–B addition reaction to unsaturated species [14,15]. It was shown that neither insertion to metal–element bonds nor reductive elimination is the rate-determining stage. Instead, ligand dissociation required for alkyne coordination was found as the rate-determining stage [14,15].

2.3. Catalytic Ar_2E_2 addition to alkynes (E = S, Se)

Recently we have investigated the catalytic reaction of E–E bond addition to alkynes with palladium catalyst formed in situ from the $Pd(PPh_3)_2Cl_2$ and Ph_2E_2–$NaBH_4$ [10]. Using this synthetic approach a moderate ca. 60% yields of the products were obtained. In the present article we concentrate on improved catalyst preparation scheme based on PhEH–Et_3N substitution reaction.

Without Et_3N the reaction does not result in the product formation (entry 2, Table 3). In the presence of base and PhEH the palladium complex shows desired catalytic activity (entry 3, Table 3). Interestingly, the yield of the product is increasing upon addition of PPh_3 to the reaction mixture (entries 3–6, Table 3) and even tenfold excess of the ligand does not lower the yield. The result is somewhat surprising, since it is generally accepted that an excess of the ligand blocks the catalytic cycle occupying coordination vacancy required to bind an alkyne molecule.

Catalytic reaction yields (entries 2–6, Table 3) are in a good qualitative agreement with dinuclear complexes concentration measured at the catalyst preparation stage (Table 2). In the absence of PPh_3 a brown precipitate insoluble in common organic solvents is formed, suggesting that catalyst polymerization to **7** takes place (Scheme 2). Polymeric palladium sulfide $[Pd(SPh)_2]_n$ formation has been reported in $Pd(OAc)_2$ reaction with PhSH [16]. In the presence of an excess of PPh_3 no brown precipitate is formed in Ph_2S_2 addition reaction and the catalytic process is carried out under homogeneous conditions.

In the entries 3–6 (Table 3) the by-product of PhSH addition to alkynes, namely $H_2C{=}C(SPh)R$, was also obtained as a trace impurity. Decreasing an amount of PhSH needed for the substitution reaction makes it possible to suppress the by-product formation without noticeable lowering of reaction yield (cf. entries 5 and 7, Table 3). We have found that the ratio $PdCl_2(PPh_3)_2$–PhEH–Et_3N = 1:1.9:3 is the most reliable for the studied reactions.

Phospine ligand effect was observed for several alkynes (entries 4–11, Table 3). For Ar_2Se_2 addition reaction 6 equivalents of PPh_3 should be added to perform the reaction in homogeneous conditions (entries 14–18, Table 3). In the presence of an excess of the phosphine ligand a very good yield was obtained for all the studied alkynes. We have found that Se–Se bond is less reactive than S–S bond within the studied catalytic reaction and in average requires longer reaction time (40 vs. 15 h) to achieve a good yield. It's interesting to note, that cyclopropyl ring is not effected during the catalytic reaction and Ph_2E_2 addition to cyclopropylacetylene resulted exclusively in formation of **9E** and **10E** (entries 13 and 16, Table 3).

The reaction can be successfully performed in toluene and benzene solutions with the product yields of 98% and 95%, respectively (see entry 5, Table 3 for reaction conditions). Using THF and acetonitryl as solvents resulted in the lower yields of 68 and 65%, respectively.

A stepwise addition of Ph_2S_2 was observed in the case of heptadiyne-1,6 (Scheme 4). Depending on the alkyne:Ph_2S_2 ratio both **16** and **17** can be synthesized in good yields. Under studied reaction conditions we did not observe cyclic products as was reported for some other E–E bond addition reactions to diynes [2].

Several ligands were tested in the catalytic reaction (Table 4). Triphenylphosphine was found as the best ligand for the reaction. A slightly lower yield was obtained with electrondeficient P(*p*-F Ph)$_3$ ligand, while electrondonor cyclohexyl (Cy) and *n*-Bu substituted

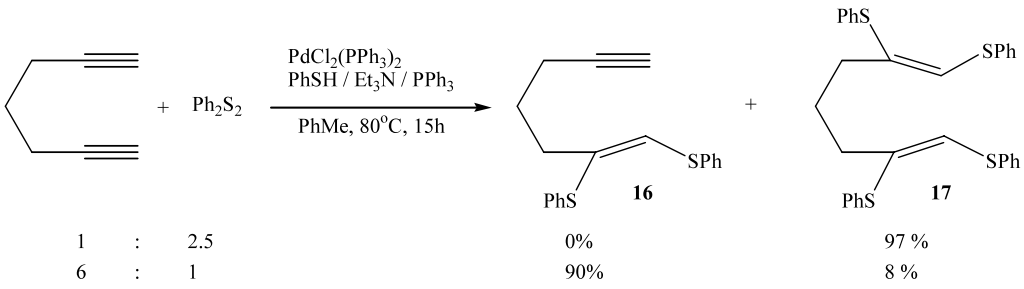

Scheme 4.

Table 4
Catalytic Ph_2S_2 addition to HC≡CCH_2CH_2OH (**13B**) utilizing different ligands in transition metal complex [a]

No.	Catalyst	Yield [b] (%)
1	$PdCl_2(PPh_3)_2$–PhSH–Et_3N–$2PPh_3$	78
2	$PdCl_2(PPh_3)_2$–PhSH–Et_3N	55
3	$PdCl_2$(DPPB)–PhSH–Et_3N	40
4	$PdCl_2(PCy_3)_2$–PhSH–Et_3N	15 [c]
5	$PdCl_2$(DPPE)–PhSH–Et_3N	0
6	$PdCl_2(CH_3CN)_2$–PhSH/Et_3N	0
7	Pd_2dba_3/$8PPh_3$	77
8	Pd_2dba_3/8P(*p*-F Ph)$_3$	74
9	Pd_2dba_3/$8Pbu_3$	2

[a] The reactions were performed in 1 mmol scale with 1.2:1 ratio of **13B**:Ph_2S_2 using 3 mol% of palladium catalyst; $PdCl_2(L)_2$–PhEH–Et_3N = 1:1.9:3. The reactions were carried out in the toluene solution (0.5 ml) at 80 °C for 15 h.
[b] Determined with NMR spectroscopy.
[c] Unknown products were also obtained with the yield ca. 15%.

phosphine ligands give very poor results. It was shown that palladium selenide complex with P(*n*-Bu)$_3$ ligand possesses mononuclear state $[Pd(SePh)_2(P(n\text{-}Bu)_3)_2]$ [17] as well as the complexes with chelate ligands [18]. Therefore, dinuclear complex formation most likely is the crucial factor for maintaining the catalytic activity. The results are in agreement with our previous study [10].

The dinuclear complexes $[Pd_2(EPh)_4(PPh_3)_2]$ can be used for catalyzing any Ph_2E_2 addition reaction to alkynes (E,E′ = S, Se). Particularly, for Ph_2S_2 addition reaction both $[Pd_2(SPh)_4(PPh_3)_2]$ and $[Pd_2(SePh)_4(PPh_3)_2]$ can serve as catalyst (Scheme 5A). In the latter case lower yield is observed (86% vs 97%) and additional selenium-containing alkenes are formed (12%). In the same way, both $[Pd_2(SPh)_4(PPh_3)_2]$ and $[Pd_2(SePh)_4(PPh_3)_2]$ can be utilized for catalytic Ph_2Se_2 addition to C≡C bond and in the former case sulfur-containing by-products are formed (Scheme 5B). These results confirm labile nature of dinuclear complexes under catalytic reaction conditions. Moreover, either $[Pd_2(SPh)_4(PPh_3)_2]$ or $[Pd_2(SePh)_4(PPh_3)_2]$ can be used as the universal catalyst for S–S and Se–Se bonds addition reactions to alkynes.

2.4. X-ray study of 9-C·HOOC–COOH

Recently we have reported the X-ray structure of $H(SePh)C{=}C(SePh)CH_2N^+HMe_2{\cdot}HOOC{-}COO^-$, which was prepared by Ph_2Se_2 addition to HC≡CCH_2NMe_2 and crystallized as 1:1 oxalic acid salt [10]. In the present study we successfully applied this methodology for preparing X-ray quality single crystals of the $H(SPh)C{=}C(SPh)CH_2N^+HMe_2{\cdot}HOOC{-}COO^-$ (**9**-C·HOOC–COOH). Molecular structure of the compound is shown on Fig. 3, main geometric parameters are listed in Table 5. Alkene unit possesses typical geometry for sp^2 hybridized atoms, with C=C distance of 1.313(4) Å and S–C=C–S dihedral angle of only 2.3°. The C=C–S bond angles of 121.5(3) and 124.3(3)° are close to expected values of 120°. Two sulfur atoms are located at the 1.748(3) and 1.759(3) Å distances from the C1 and C2 vinyl atoms, respectively. According to the bond angles C2-S1–C5 = 99.37(15) and C1–S2–C11 = 103.12(16)° the phenyl rings should not cause large sterical hindrance for external coordination to the sulfur atoms. Therefore, the compound possesses favorable conformation for considering it as chelate ligand. The similar conformation has been found for the selenium analog [10] suggesting this could be a general property of the *Z*-bis-(sulfur–selenium)substituted alkenes. The S···S distance in **9**-C·HOOC–COOH −3.220(1) Å is by 0.081 Å shorter than the Se···Se distance found in X-ray structure of the selenium analog [10].

3. Conclusions

The mechanistic study has shown that catalytic addition of both S–S and Se–Se bonds to alkynes involves dinuclear palladium complexes. Neither an alkyne insertion into the Pd–E bond nor a C–E reductive elimination was proved to be a rate-determining stage of the catalytic cycle. Since an oxidative addition of S–S and Se–Se bonds to Pd(0) is also very fast and the nature of alkyne is rather important, most

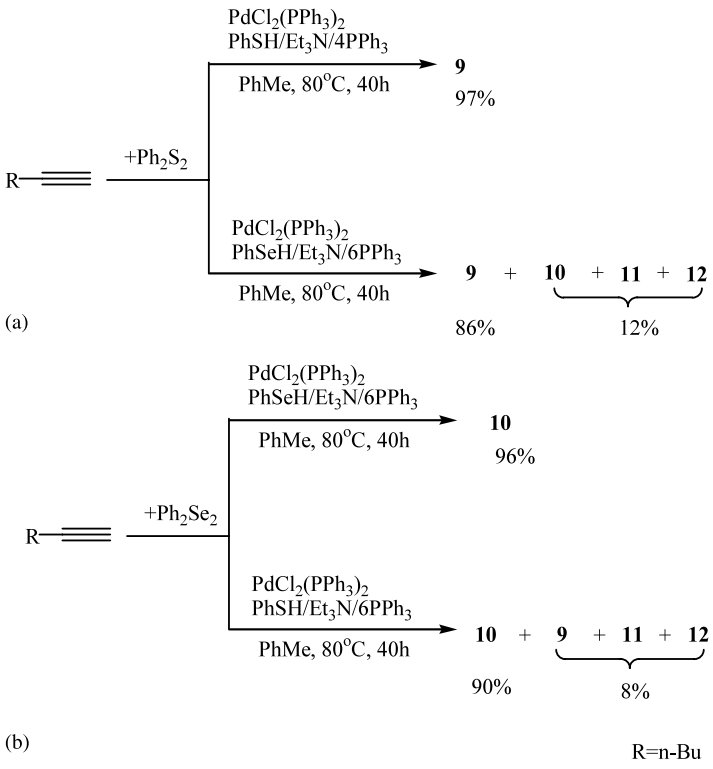

Scheme 5.

probably the rate-determining stage of the catalytic cycle is an alkyne coordination or a dissociation of the dinuclear complex accompanied with alkyne coordination. The conclusion is in agreement with theoretical findings [14,15].

An unusual phosphine ligand effect of increasing the yield of the catalytic reaction was found in the studied system. Most likely an excess of the ligand suppresses polymerization of palladium complexes maintaining the catalyst in the active state. In the studied reaction conditions an excess of phosphine ligand does not retard in significant manner coordination of alkyne to palladium complex.

A new synthetic procedure was developed for the stereoselective Ar_2E_2 (E = S, Se) addition to alkynes using easily available palladium complex and the scope of the reaction was investigated. Our study has shown that under palladium catalyzed conditions S–S bond is more reactive toward alkynes compared to Se–Se bond. Possible explanation of lower reactivity in Se–Se bond addition reaction is the higher stability of palladium complexes with bridged SePh ligands. X-ray study of *Z*-bis-(PhS)-substituted alkene showed favoring geometry for the possible application of the synthesized products as chelate ligands.

4. Experimental

4.1. General

Unless otherwise stated, synthetic work was carried out under argon atmosphere. The reagents were obtained from commercial sources (Aldrich, Acros) and checked by NMR before usage.

4.2. NMR Spectroscopy

All NMR measurements were performed using a three channel Bruker DRX500 spectrometer operating at 500.1, 202.5, 125.8 and 95.4 MHz for ^{1}H, ^{31}P, ^{13}C and ^{77}Se nuclei respectively. All 2D spectra were recorded using inverse triple resonance probehead with active shielded *Z*-gradient coil. ^{1}H and ^{13}C chemical shifts are reported relative to the corresponding solvent signals used as internal reference, external 85% H_3PO_4–H_2O ($\delta = 0.0$ ppm) used for ^{31}P and Ph_2Se_2–$CDCl_3$ ($\delta =$ 463.0 ppm) for ^{77}Se [19].

4.2.1. 2D ^{1}H–^{77}Se HMQC NMR experiment

The spectrum was collected with ^{1}H and ^{77}Se 90° pulses of 12.5 and 16.0 μs, respectively, a relaxation delay of 2 s, $\Delta = (2 \cdot J_{H-Se})^{-1} = 250$ ms (optimized for

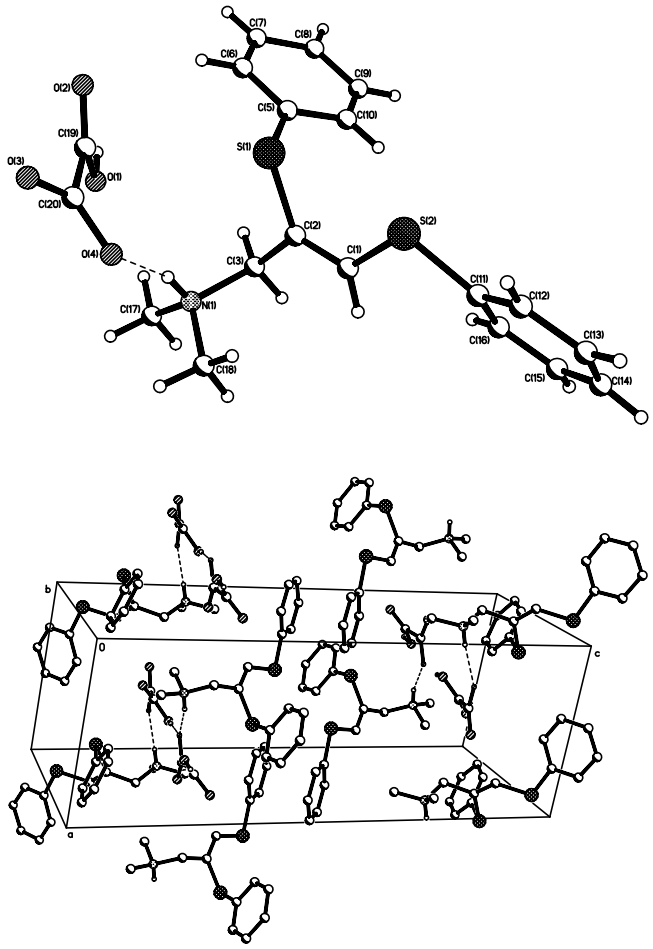

Fig. 3. Molecular structure (top) and crystal packing (bottom) for $HC(SPh)=C(SPh)CH_2N^+HMe_2\cdot HOOC-COO^-$ (**9-C**·HOOC–COOH).

long range coupling constant of 2 Hz), a 0.25 s acquisition time and 4500 and 25000 Hz spectral windows for the ^1H(F2) and ^{77}Se(F1) dimensions correspondingly. Four or eight transients were averaged for each of 256 increments on t_1. The data was zero filled to 2048x2048 matrix and processed with QSINE(SSB = 2) window function for both F2 and F1 dimensions. The 1 ms sine shaped pulse field gradient pulses with the ratio 50.0:30.0:35.3 (%) followed with 100 μs recovery delay were applied.

4.2.2. 2D NOESY NMR experiment

The spectra were recorded using bipolar gradient pulse sequence: $90-t_1-90-\tau_{mix}/2-G1-180-G2-\tau_{mix}/2-90-acq$, with $\tau_{mix} = 1-2$ s and 40.0, −40.0 (%) field gradient pulses for G1 and G2, respectively. The further details as described earlier [20].

The rest of NMR experiments were performed using pulse sequences supplied by hardware manufacturer.

Table 5
Selected Bond lengths (Å) and bond angles (°) for **9C**

Bond lengths			
S(1)–C(2)	1.759(3)	C(5)–C(6)	1.376(5)
S(1)–C(5)	1.776(4)	C(5)–C(10)	1.394(5)
S(2)–C(1)	1.748(3)	C(6)–C(7)	1.370(6)
S(2)–C(11)	1.773(3)	C(7)–C(8)	1.399(6)
O(1)–C(19)	1.301(4)	C(8)–C(9)	1.377(6)
O(2)–C(19)	1.196(4)	C(9)–C(10)	1.363(6)
O(3)–C(20)	1.220(3)	C(11)–C(12)	1.377(5)
O(4)–C(20)	1.264(3)	C(11)–C(16)	1.384(5)
N(1)–C(17)	1.480(4)	C(12)–C(13)	1.390(6)
N(1)–C(18)	1.486(4)	C(13)–C(14)	1.356(6)
N(1)–C(3)	1.505(4)	C(14)–C(15)	1.412(7)
C(1)–C(2)	1.313(4)	C(15)–C(16)	1.359(5)
C(2)–C(3)	1.519(4)	C(19)–C(20)	1.549(4)
Bond angles			
C(2)–S(1)–C(5)	99.37(15)	C(10)–C(9)–C(8)	119.1(4)
C(1)–S(2)–C(11)	103.12(16)	C(9)–C(10)–C(5)	121.1(4)
C(17)–N(1)–C(18)	110.5(3)	C(12)–C(11)–C(16)	119.1(3)
C(17)–N(1)–C(3)	110.8(2)	C(12)–C(11)–S(2)	117.1(3)
C(18)–N(1)–C(3)	111.9(2)	C(16)–C(11)–S(2)	123.6(3)
C(2)–C(1)–S(2)	124.3(3)	C(11)–C(12)–C(13)	120.6(4)
C(1)–C(2)–C(3)	121.8(3)	C(14)–C(13)–C(12)	119.4(4)
C(1)–C(2)–S(1)	121.5(3)	C(13)–C(14)–C(15)	120.7(4)
C(3)–C(2)–S(1)	116.7(2)	C(16)–C(15)–C(14)	118.7(4)
N(1)–C(3)–C(2)	114.0(2)	C(15)–C(16)–C(11)	121.3(4)
C(6)–C(5)–C(10)	119.1(4)	O(2)–C(19)–O(1)	125.3(3)
C(6)–C(5)–S(1)	120.0(3)	O(2)–C(19)–C(20)	121.9(3)
C(10)–C(5)–S(1)	120.8(3)	O(1)–C(19)–C(20)	112.7(3)
C(7)–C(6)–C(5)	120.9(4)	O(3)–C(20)–O(4)	126.6(3)
C(6)–C(7)–C(8)	118.8(4)	O(3)–C(20)–C(19)	117.5(3)
C(9)–C(8)–C(7)	120.9(4)	O(4)–C(20)–C(19)	115.8(2)

4.3. Ph_2E_2 oxidative addition to $Pd(PPh_3)_4$ ($E = S, Se$)

Ph_2E_2 (3.8×10^{-5} mol) was dissolved in 0.4 ml of toluene and $Pd(PPh_3)_4$ (22.0 mg, 1.9×10^{-5} mol) was added to the solution. The solution was heated with stirring at 80 °C for 10 min and cooled to the room temperature (r.t.). Before recording NMR spectra 0.1 ml of C_6D_6 was added to the mixture.

4.4. Preparation of mixed complexes (**8**)

4.4.1. Method A

Separately prepared (see Section 4.3) solutions of dinuclear complexes **3**, **4** and **5**, **6** were mixed and heated with stirring at 80 °C for 10 min. The solution was cooled to the r.t. before recording NMR spectra.

4.4.2. Method B

Ph_2S_2 (8.3 mg, 3.8×10^{-5} mol) and Ph_2Se_2 (11.9 mg, 3.8×10^{-5} mol) were dissolved in 0.8 ml of toluene and $Pd(PPh_3)_4$ (44.0 mg, 3.8×10^{-5} mol) was added to the solution. The solution was heated with stirring at 80 °C for 10 min and cooled to the r.t. Before recording NMR spectra 0.2 ml of C_6D_6 was added to the mixture.

4.5. Alkyne insertion reaction

To each of the solutions of 3.8×10^{-5} mol of complexes **3**, **4** and **5**, **6** (see Section 4.3) and **8** (see Section 4.4) in 0.5 ml of toluene the alkyne (7.6×10^{-5} mol) was added and heated with stirring at 80 °C for 2 h. The solutions were cooled to the r.t. and the solvent was removed on rotor evaporator. The products were extracted with 0.5 ml of $CDCl_3$.

4.6. General synthetic procedure

4.6.1. Method A—using $Pd(PPh_3)_2Cl_2$ as a catalyst

Ar_2E_2 (1.0×10^{-3} mol) was dissolved in 2.0 ml of toluene followed by addition of: (i) $PdCl_2(PPh_3)_4$ (21.1 mg, 3.0×10^{-5} mol); (ii) PPh_3 (31.5 mg, 1.2×10^{-4} mol for E = S and 47.2 mg, 1.8×10^{-4} mol for E = Se); (iii) PhEH (5.7×10^{-5} mol, diluted solution in 0.1 ml of toluene); (iv) Et_3N (9.1 mg, 9.0×10^{-5} mol). The mixture was stirred upon complete dissolving of palladium complex and forming homogeneous dark brown solution. The alkyne (1.2×10^{-3} mol) was added and reaction mixture was heated at 80 °C in a sealed tube (15 h E = S, 40 h E = Se). After completing the reaction the product was further purified with chromatography on silica.

4.6.2. Method B—using $Pd(PPh_3)_4$ as a catalyst

An earlier published [9] procedure was used except an additional amounts of PPh_3 (two and four equivalents for E = S and E = Se, respectively) were added and the reaction was performed in a sealed tube. The reaction was performed with 3 mol% of palladium catalyst and alkyne:Ar_2E_2 = 1.2:1 ratio.

Compounds **10B**, **9B** [9] and **10C** [10] were identified according to published data. Structure elucidation for the other compounds was made utilizing two-dimensional NOESY, LR-COSY, ^1H-^{13}C HSQC, ^1H-^{13}C HMBC experiments. For the selenium-containing products two-dimensional ^1H–^{77}Se HMQC NMR experiment was performed. Compound **16** (Scheme 4) was obtained as unseparable **16**:**17** mixture and identified with the above set of NMR experiments.

4.6.3. Z-HC(SPh)=C(SPh)–C_6H_{10}(OH) (**9A**)

Yellow oil. ^1H ($CDCl_3$; δ, ppm): 7.39 (m, 2H, Ph), 7.34 (s, 1H, HC=), 7.33–7.21 (m, 7H, Ph), 7.13 (m, 1H, Ph), 1.80–1.50 (m, 9H, CH_2), 1.64 (m, 1H, $^{1/2}CH_2$). $^{13}C\{^1H\}$ ($CDCl_3$; δ, ppm): 138.2, 135.5, 135.1, 130.5, 129.1, 128.9, 127.3, 126.8, 125.4, 75.8, 36.3, 25.2, 21.8. Anal. Found: C, 70.20; H, 6.76; S, 18.53. Calc. for $C_{20}H_{22}OS_2$: C, 70.13; H, 6.47; S, 18.72%. MS (EI), *m/e* 342 (M^+).

4.6.4. Z-HC(SPh)=C(SPh)–CH_2–NMe_2·HOOC–COOH (**9**-C·HOOC–COOH)

White solid. After completing the reaction and removing the solvent and unreacted alkyne on rotor evaporator the crude was dissolved in 3 ml of toluene. The solution of HOOC–COOH in 2 ml of THF (1:1 to **9C**) was added resulting in immediate white precipitate formation. The solid was washed with toluene, THF, extracted with 4 ml of methanol and dried in vacuum.

^1H (CD_3OD; δ, ppm): 7.62 (s, 1H, HC=), 7.52 (m, 2H, Ph), 7.44–7.27 (m, 8H, Ph), 3.87 (s, 2H, –CH_2–), 2.83 (s, 6H, CH_3–). $^{13}C\{^1H\}$ (CD_3OD; δ, ppm): 166.2, 149.9, 134.7, 133.2, 131.9, 130.8, 130.7, 130.6, 129.4, 128.8, 118.9, 62.1, 43.1. Anal. Found: C, 58.11; H, 5.46; N, 3.53; S, 16.16. Calc. for $C_{19}H_{21}NO_4S_2$: C, 58.29; H, 5.41; N, 3.58; S, 16.38. MS (EI), *m/e* 301 (M^+ – HOOC–COOH).

4.6.5. Z-HC(SPh)=C(SPh)–$^{\alpha}CH_2$–$^{\beta}CH_2$–$^{\gamma}CH_2$–$^{\delta}CH_3$ (**9D**)

Light oil. ^1H ($CDCl_3$; δ, ppm): 7.41 (m, 2H, Ph), 7.37 (m, 2H, Ph), 7.34–7.18 (m, 6H, Ph), 6.56 (s, 1H, HC=), 2.25 (t, 2H, J = 7.7 Hz, –$^{\alpha}CH_2$–), 1.48 (tt, 2H, J_1 = 7.7 Hz, J_2 = 7.5 Hz, –$^{\beta}CH_2$–), 1.25 (tq, 2H, J_1 = 7.3 Hz, J_2 = 7.5 Hz, –$^{\gamma}CH_2$–), 0.83 (t, 3H, J = 7.3 Hz, –$^{\delta}CH_3$). $^{13}C\{^1H\}$ ($CDCl_3$; δ, ppm): 135.9, 134.3, 133.8, 130.5, 129.7, 129.1, 129.0, 128.9, 126.8, 126.7, 36.8, 30.7, 21.9, 13.8. Anal. Found: C, 71.99; H, 6.68; S, 21.08. Calc. for $C_{18}H_{20}S_2$: C, 71.95; H, 6.71; S, 21.34%. MS (EI), *m/e* 300 (M^+).

4.6.6. Z-HC(SPh)=C(SPh)–C_3H_5 (**9E**)

Light oil. ^1H ($CDCl_3$; δ, ppm): 7.38 (m, 4H, Ph), 7.32–7.16 (m, 6H, Ph), 6.62 (s, 1H, HC=), 1.61 (q, 1H, CH), 0.60 (d, 4H, CH_2). $^{13}C\{^1H\}$ ($CDCl_3$; δ, ppm): 135.7, 134.5, 134.4, 129.8, 129.7, 129.0, 128.8, 126.9, 126.4, 18.3, 6.6. Anal. Found: C, 71.95; H, 5.72; S, 22.42. Calc. for $C_{17}H_{16}S_2$: C, 71.78; H, 5.67; S, 22.55. MS (EI), *m/e* 284 (M^+).

4.6.7. Z-HC(SePh)=C(SePh)–C_3H_5 (**10E**)

Light oil. ^1H ($CDCl_3$; δ, ppm): 7.54 (m, 4H, Ph), 7.27 (m, 6H, Ph), 6.97 (br s, 1H, HC=), 1.60 (m, 1H, CH), 0.58 (m, 4H, CH_2). $^{13}C\{^1H\}$ ($CDCl_3$; δ, ppm): 137.2, 132.6, 132.4, 131.2, 129.9, 129.2, 129.1, 127.4, 127.2, 127.1, 20.5, 7.2. Anal. Found: C, 54.02; H, 4.29; Se, 41.89. Calc. for $C_{17}H_{16}Se_2$: C, 53.98; H, 4.26; S, 41.75%. MS (EI), *m/e* 380 (M^+).

4.6.8. Z-(p-MePhSe)HC=C(p-MePhSe)–CH_2–CH_2OH (**14B**)

Yellow oil, solidified on cooling. ^1H ($CDCl_3$; δ, ppm): 7.44 (m, 4H, Ar), 7.10 (m, 4H, Ar), 6.99 (s, 1H, HC =), 3.66 (t, 2H, J = 6.2 Hz, CH_2OH), 2.47 (t, 2H, J = 6.0 Hz, CH_2), 2.33 (s, 3H, CH_3), 2.32 (s, 3H, CH_3). $^{13}C\{^1H\}$ ($CDCl_3$; δ, ppm): 137.7, 137.6, 133.4, 133.1, 131.1,

131.0, 130.1, 130.0, 61.0, 42.5, 21.1, 21.0. ^{77}Se ($CDCl_3$; δ, ppm): 395.3, 374.0. Anal. Found: C, 52.72; H, 4.98; Se, 38.42. Calc. for $C_{18}H_{20}OSe_2$: C, 52.70; H, 4.91; Se, 38.49. MS (EI), *m/e* 412 (M^+).

4.6.9. *Z*-(*p*-F PhSe)HC=C(*p*-F PhSe)–CH_2–CH_2OH (**15B**)

Yellow oil, solidified on cooling. ^{1}H ($CDCl_3$; δ, ppm): 7.53 (m, 4H, Ar), 6.99 (m, 4H, Ar), 6.97 (s, 1H, HC=), 3.69 (t, 2H, $J = 6.2$ Hz, CH_2??), 2.48 (t, 2H, $J = 6.0$ Hz, CH_2). ^{13}C{^{1}H} ($CDCl_3$; δ, ppm): 163.6, 161.7, 135.3, 135.2, 135.1, 131.4, 131.3, 125.1, 125.0, 123.5, 123.4, 116.7, 116.6, 116.5, 116.4, 61.0, 42.5. ^{77}Se ($CDCl_3$; δ, ppm): 398.5, 375.6. Anal. Found: C, 46.23; H, 3.45; Se, 37.85. Calc. for $C_{16}H_{14}F_2OSe_2$: C, 45.95; H, 3.37; Se, 37.76%. MS (EI), *m/e* 420 (M^+).

4.6.10. *Z,Z*-HC(SPh)=C(SPh)–$^{\alpha}CH_2$–$^{\beta}CH_2$–$^{\alpha}CH_2$–(SPh)C=CH(SPh) (**17**)

Yellow oil. ^{1}H ($CDCl_3$; δ, ppm): 7.36 (m, 4H, Ph), 7.33–7.15 (m, 16H, Ph), 6.49 (s, 2H, HC=), 2.18 (t, 4H, $J = 7.3$ Hz, –$^{\alpha}CH_2$–), 1.70 (m, 2H, $J = 7.3$ Hz, –$^{\beta}CH_2$–). ^{13}C{^{1}H} ($CDCl_3$; δ, ppm): 135.6, 133.5, 133.2, 130.5, 130.0, 129.7, 129.0, 128.9, 126.9, 126.8, 36.0, 27.3. Anal. Found: C, 70.30; H, 5.32; S, 24.18. Calc. for $C_{31}H_{28}S_4$: C, 70.41; H, 5.34; S, 24.25. MS (EI), *m/e* 528 (M^+).

4.7. Crystal structure determination

Single crystals of **9**-C·HOOC–COOH were obtained by slow evaporation of methanol solution. The samples were mounted in air on glass fiber using 5 min epoxy resin. The X-ray intensity data sets were collected on a Bruker AXS SMART 1000 diffractometer equipped with a CCD detector (graphite monochromator, 230(2)K, ω scanning technique, scan step was 0.3°, frames were exposed for 30 s) using a standard procedure [21]. The semiempirical absorption correction was applied [22]. The crystallographic parameters and selected details of the refinement of structures are given in Table 6. The main geometric parameters are given in Table 5. The structures were solved by direct and Fourier techniques, and refined by full-matrix least-squares method with anisotropic thermal parameters for all non-hydrogen atoms. The positions of the hydrogen atoms of the phenyl, methyl and methylene substituents were calculated geometrically and refined using the riding model. The positions of the other hydrogen atoms were found from the difference Fourier map. All calculations were carried out with the use of the SHELEX-97 program package [23].

Table 6
Data collection and processing parameters for the compounds **9**-C·HOOC–COOH

Empirical formula	$C_{19}H_{21}NO_4S_2$
Formula weight	391.49
Temperature (K)	293(2)
Wavelength (Å)	0.71069
Crystal system	Monoclinic
Space group	$P2_1/n$
Unit cell dimensions	
a (Å)	8.376(2)
b (Å)	10.447(2)
c (Å)	22.842(5)
α (°)	90
β (°)	95.72(3)
γ (°)	90
V (A^3)	1988.8(7)
Z	4
D_{calc} (Mg m^{-3})	1.307
Absorption coefficient (mm^{-1})	0.291
F(000)	824
Theta range for data collection (°)	1.79–29.96
Index ranges	$-11 \le h \le 11$, $0 \le k \le 14$, $0 \le l \le 31$
Reflections collected/unique	5771/5771 [$R_{int} = 0.0760$]
Completeness to theta = 29.96 (%)	94.9
Absorption correction	Psi-scan
Max. and min. transmission	0.675 and 0.983
Refinement method	Full-matrix least-squares on F^2
Data/restraints/parameters	5771/0/243
Goodness-of-fit on F^2	1.000
Final R indices [2359$I > 2\sigma(I)$]	$R_1 = 0.0686$, $wR_2 = 0.1585$
R indices (all data)	$R_1 = 0.1726$, $wR_2 = 0.2108$
Largest difference peak and hole (e A^{-3})	1.093 and −0.388

5. Supplementary material

Crystallographic data for the structural analysis have been deposited with the Cambridge Crystallographic Data Centre, CCDC no. 212256. Copies of this information may be obtained free of charge from The Director, CCDC, 12 Union Road, Cambridge CB2 1EZ, UK (Fax: +44-1223-336033; e-mail: deposit@ccdc.cam.ac.uk or www: http://www.ccdc.cam.ac.uk).

Acknowledgements

The work was carried out with partial support from the Chemistry and Material Science Branch of the Russian Academy of Sciences (Program: 'Theoretical and experimental investigations of the nature of chemical bonding and mechanisms of the most important chemical reactions and processes'). X-ray diffraction analysis was performed at the Center of X-ray Diffraction Studies, A.N. Nesmeyanov Institute of Organoelement Compounds, Russian Academy of Sciences, Moscow.

References

[1] A. Togni, H. Grützmacher (Eds.), Catalytic Heterofunctionalization, Wiley–VCH, Weinheim, 2001.
[2] I.P. Beletskaya, C. Moberg, Chem. Rev. 99 (1999) 3435.
[3] T. Wirth (Ed.), Organoselenium Chemistry: Modern Developments in Organic Synthesis, Springer-Verlag, Berlin, 2000.
[4] T.G. Back (Ed.), Organoselenium Chemistry: A Practical Approach, Oxford University Press, New York, 1999.
[5] C. Paulmier, Selenium Reagents and Intermediates in Organic Synthesis, Pergamon Press, Oxford, 1986.
[6] S. Patai, Z. Rappoport (Eds.), The Chemistry of Organic Selenium and Tellurium Compounds, vols. 1–2, Wiley, New York, 1986.
[7] P.I. Clemenson, Coord. Chem. Rev. 190 (1990) 171.
[8] C. Lauterbach, J. Fabian, Eur. J. Inorg. Chem. (1999) 1995 and references therein.
[9] H. Kuniyasu, A. Ogawa, S.-I. Miyazaki, I. Ryu, N. Kambe, N. Sonoda, J. Am. Chem. Soc. 113 (1991) 9796.
[10] V.P. Ananikov, I.P. Beletskaya, G.G. Aleksandrov, I.L. Eremenko, Organometallics 22 (2003) 1414.
[11] R. Zanella, R. Ros, M. Graziani, Inorg. Chem. 12 (1973) 2736.
[12] I. Nakanishi, S. Tanaka, K. Matsumoto, S. Ooi, Acta Crystallogr. Sect. C 50 (1994) 58.
[13] R. Oilunkaniemi, R.S. Laitinen, M. Ahlgren, J. Organomet. Chem. 623 (2001) 168.
[14] Q. Cui, D.G. Musaev, K. Morokuma, Organometallics 16 (1997) 1355.
[15] Q. Cui, D.G. Musaev, K. Morokuma, Organometallics 17 (1998) 742.
[16] A. Ogawa, J. Organomet. Chem. 611 (2000) 463.
[17] E.C. Alyea, G. Ferguson, S. Kannan, Polyhedron 17 (1998) 2231.
[18] V.K. Jain, S. Kannan, R.J. Butcher, J.P. Jasinski, J. Chem. Soc. Dalton Trans. (1993) 1509.
[19] H. Duddeck, Sulfur, selenium, & tellurium NMR, in: D.M. Grant, R.K. Harris (Eds.), Encyclopedia of Nuclear Magnetic Resonance, vol. 7, Wiley, Chichester, 1996, pp. 4623–4636.
[20] V.P. Ananikov, S.A. Mitchenko, I.P. Beletskaya, J. Organomet. Chem. 636 (2001) 175.
[21] SMART (control) and SAINT (integration) software, version 5.0 Bruker AXS Inc., Madison, WI, 1997.
[22] G.M. Sheldrick, SADABS, Program for Scaling and Correction of Area Detector Data, University of Gottingen, Göttingen, Germany, 1997.
[23] G.M. Sheldrick, Crystallographic Computing 3: Data Collection, Structure Determination, Proteins and Databases, Claredon Press, New York, 1985, p. 175.